Evaluation of Capability of Some Amino Acid-based Poly (Ionic Liquid)s as Biocompatible Agent for Co2 Absorption

Narmin Noorani (nnorani1@yahoo.com)
University of Tabriz https://orcid.org/0000-0002-8156-2018
Abbas Mehrdad
University of Tabriz

Research Article

Keywords: AAPILs, Thermodynamics, Absorption, CO2

Posted Date: December 14th, 2021

DOI: https://doi.org/10.21203/rs.3.rs-1123236/v1

Evaluation of capability of some amino acid-based poly (ionic liquid)s as biocompatible agent for CO_2 absorption

Narmin Noorani*, Abbas Mehrdad

Department of Physical Chemistry, Faculty of Chemistry, University of Tabriz, Tabriz, Iran

Abstract

In this study, seven amino acid-based poly(ionic liquid)s (AAPILs) such as poly(1-butyl-3-vinylimidazolium glycinate), P[VBIm][Gly], poly (1-butyl-3-vinylimidazolium alaninate), P[VBIm][Ala], poly(1-butyl-3-vinylimidazolium valinate), P[VBIm][Val], poly(1-butyl-3-vinylimidazolium prolinate) P[VBIm][Pro], poly(1-butyl-3-vinylimidazolium hisdinate), P[VBIm][His], poly(1-butyl-3-vinylimidazolium lysinate), P[VBIm][Lys], and poly(1-butyl-3-vinylimidazolium arginate), P[VBIm][Arg] have been synthesized, characterized, and their CO_2 absorption capacities were investigated using quartz crystal microbalance (QCM) at temperature range 288.15–308.15 and pressures up to 5 bar. Based on the absorption mechanism, the reaction equilibrium thermodynamic model is applied to correlating the experimental CO_2 absorption capacities. The reaction equilibrium constant and Henry's law constant were calculated to evaluate the efficiency of the AAPILs for CO_2 absorption. In the investigated AAPILs, the CO_2 absorption capacity was as follows: P[VBIm][Arg] > P[VBIm][Lys] > P[VBIm][His] > P[VBIm][Pro] > P[VBIm][Gly] > P[VBIm][Val] > P[VBIm][Ala]. The accessibility of available more amine groups in AAPIL with arginate anion is the main factor for the high CO_2 absorption capacity. Also, chemical absorption of CO_2 via carbamate formation was corroborated by FT-IR spectroscopy.

Keywords: AAPILs; Thermodynamics; Absorption; CO_2

*Corresponding Author,

E–mail address:nnorani1@yahoo.com

Introduction

The emission of carbon dioxide from the combustion of natural gas, petroleum, and coal is the major reason of global warming. Therefore, carbon dioxide capture and conversion are one of the major environmental concerns, in the past decade which has attracted the main attention from the scientific society [1–3]. Carbon capture and storage (CCS) is an efficient procedure to absorb carbon dioxide from such industries [4]. Various technologies for CO_2 capture are applied containing, membrane separation, chemical absorption, physical adsorption, and hybrid applications of these. Amongst the prevalent technologies of CO_2 uptake, chemical absorption with alkanolamines or their combinations such as n-methyl diethanolamine (MDEA), monoethanolamine (MEA), and diethanolamine (DEA) is one of the efficient technologies for CO_2 capture. Nevertheless, these absorbents are facing some limitations such as solvent loss, the amines degradation at high temperature in the process of regeneration, and the amines corrosion [5]. Therefore, it seriously affects the progress of the environmental process. Hence, novel materials or solvents such as ionic liquids (ILs), membranes, and solid adsorbents as good alternatives for efficacious capture of CO_2 have offered. Ionic liquids (ILs) have been attracted considerable attention as alternative CO_2 absorbents owing to their special characteristics such as strong solubility power, high thermal, high polarity, chemical stability, negligible volatility, and high affinity to acid gases [6–9]. Designing the physical and chemical properties of IL by selecting the favorable cations and anions can be caused by to increase in the CO_2 absorption capacity in ILs [10]. Davis et al. [11] investigated the CO_2 uptake with a new task-specific ionic liquid and indicate that the interactions of chemical was major effective for CO_2 absorption and molar capture of CO_2 per mole of ionic liquid approach 0.5. Khanna et al [12] reported

absorption capacity in amino acid-based ILs with 1-butyl 3-methyl imidazolium cation and they indicate that maximum CO_2 absorption with 0.62 mol CO_2/mol IL and 0.48 mol/mol are related to [bmim][Arg] and [bmim][Lys], respectively. Saravanamurgan et al [13] have surveyed CO_2 absorption onto amino acid ionic liquids with ammonium cation and various anions containing lysinate, histidinate, asparaginate, and glutaminate. They have proposed that these ILs increment CO_2 absorption capacity via chemisorptions process. Despite these advantages, amino acid ionic liquids face problems such as having lower thermal stability than common ILs. The first time, Tang et al. [14] were investigated CO_2 adsorption capacities onto polymerized ionic liquids (PILs) and reveal that PILs had further CO_2 capture than other ILs. Also, they indicated that P[VBTMA][BF_4] and P[MATMA][BF_4] have a capacity of 10.22 mol% and 7.99 mol% respectively, while their monomers, not observe CO_2 capture due to having structures of crystalline in low pressure [15]. Wilfred et al [16] have been reported that the CO_2 solubility in P[VBTMA][Cl] ~0.188 mol CO_2/mole PIL further than the monomer, [VBTMA][Cl] ~0.07mol CO_2/mole IL. Therefore, the CO_2 uptake capacity in PILs is higher than their monomeric state; this behavior is related to their size and free volume which affects their physical adsorption [17]. Polymerized ionic liquids are solid and easily controllable compared to the liquid state. The CO_2 absorption capacity relates to the polymer backbone, polycation sort, and anion type [14]; hence the PILs properties are modified by exchanging the polycation-anion pair [18]. In this study, CO_2 absorption in AAPILs with vinyl imidazolium-cation and aminate-anion was investigated. The seven AAPILs: poly (1-butyl-3-vinylimidazolium glycinate), P[VBIm][Gly], poly (1-butyl-3-vinylimidazolium alaninate), P[VBIm][Ala], poly (1-butyl-3-vinylimidazolium valinate), P[VBIm][Val], poly (1-butyl-3-vinylimidazolium prolinate) P[VBIm][Pro], poly (1-butyl-3-vinylimidazolium hisdinate), P[VBIm][His], poly (1-butyl-3-vinylimidazolium lysinate),

P[VBIm][Lys], and poly (1-butyl-3-vinylimidazolium arginate), P[VBIm][Arg] were synthesized by the neutralization technique and characterized using proton nuclear magnetic resonance (^{1}HNMR). CO_2 absorption in AAPILs was evaluated in temperature range 288.15–308.15 K and pressures up to 5 bar using quartz crystal microbalance (QCM). The measured CO_2 absorption was fitted by the reaction equilibrium thermodynamic model (RETM) based on the absorption mechanism presuming the complexes formation. The corresponding thermodynamic parameters, contain Henry's law constant (H) and reaction equilibrium constant (K_x) were calculated. The molar enthalpy the CO_2 solution was determined from the absorption data and thermodynamics theory. The chemical adsorption of CO_2 due to formation of carbamate has been corroborated by spectroscopy of fourier transform infrared (FT-IR). The effect of anion in the poly(ionic liquid)s on the CO_2 absorption capacity has been surveyed.

Experimental Section

Materials

1–vinylimidazole (>99% wt%), L-Glycine (Gly), α-Alanine (Ala), L–Proline (Pro), L-Valine (Val), L–Histidine (His), L-Lysine (Lys), and L–Arginine (Arg) were provided from Sigma Aldrich products (purity ≥ 99.99 wt%). 2,2′–Azobis (2–ethylpropionitrile) (AIBN) as initiator, 1–Bromobutane (>99% wt%), Dimethylformamide (purity > 0.99 wt%), Ethyl acetate (purity > 0.99 wt%), acetone and Ethanol (purity ≥ 99.99 wt%) were purchased from Merck. The molecular structure of amino acids and their properties are illustrated in Table 1. CO_2 (purity ≥ 99.99 wt%) was used in gas absorption experiments.

Synthesis

Synthesis of Ionic Liquid

The ionic liquid, 1–butyl–3–vinyl imidazolium bromide, [VBIm][Br] was synthesized by the reported methods in the literatures [19,20] via direct alkylation of 1-vinyl imidazole by an excess value of 1-bromobutane refluxed at 350 K for 48 hours under an argon atmosphere. Then the obtained product was extracted by ethyl acetate. To eliminate ethyl acetate and 1-bromobutane, the product was dried at 318 K by a rotary evaporator. To assurance the elimination of remaining ethyl acetate and 1-bromobutane, the formed IL was exposed at high vacuum condition for at least 12 h. The ionic liquid was utilized after vacuum desiccated for 72 h to eliminate the moisture. The water content of ionic liquid was determined with Karl-Fischer titrator (720-KSS-Metrohm Herisau, Switzerland) and it was less than 0.01 in mass fraction. The synthesized ionic liquid were characterized by ^{1}HNMR (Bruker Av-400, Germany) and FT-IR.

^{1}H NMR (400 MHz, $CDCl_3$, δ_H, ppm): 10.95 (s, 1H, NCHN), 7.89 (t, 1H, NCHC), 7.63(t, 1H, CCHN), 7.50 (dd, 1H, CH_2CHN), 5.95 (dd, 1H, HCHCHN), 5.36 (dd, 1H, HCHCHN), 4.38 (t, 2H, NCH_2C), 1.91 (m, 2H, $CH_2CH_2CH_2$), 1.37 (m, 2H, $CH_2CH_2CH_3$), 0.96 (t, 3H, CH_2CH_3). FT-IR (ν_{max}, cm^{-1}): 3145, 3072 (CH imidazole ring), 2964, 2935, 2870 (CH aliph), 1652 (C=C), 1571, 1551 (CH imidazole ring).

Synthesis of amino acid-based polyionic liquids (AAPILs)

To synthesis of poly(1-butyl-3-vinylimidazolium aminate), P[VBIm][AA] with different aminates (glycinate $[Gly]^-$, alaninate $[Ala]^-$, valinate $[Val]^-$, prolinate $[Pro]^-$, hisdinate $[His]^-$, lysinate $[Lys]^-$, and arginate $[Arg]^-$), firstly, poly(1-butyl-3-vinylimidazolium bromide), P[VBIm][Br] was synthesized using refluxing the mixture of [BVIm][Br] (0.131 mol) and AIBN (0.152 mmol) in DMF (50 mL) at 338 K for 24 h under a argon atmosphere [21]. P[VBIm][Br] was separated via precipitation in acetone and filtering the synthesized product. Poly(1-butyl-3-vinyl imidazolium bromide) was dried at high vacuum condition for at least 12h.

P[VBIm][Br] characterized using the ^{1}HNMR and FT-IR. ^{1}HNMR and FT-IR spectra of P[VBIm][Br] is displayed in the supplementary information (Fig.S1 and S2). Then, poly(1-butyl-3-vinyl imidazolium hydroxide) (P[VBIm][OH]) was procured from aqueous solution of P[VBIm][Br] through anion exchange resin. The exchange of bromide anion with hydroxide was carried out in the glass column contains ion exchange resin and residual Br^- was tested with silver nitrate ($AgNO_3$). Prepared P[VBIm][OH] aqueous solution was added drop wise to excess equimolar aqueous L-Glycine, α-Alanine, L-Valine, L–Proline, L–Histidine, L-Lysine, or L–Arginine (1.2 equivalent) solutions, and stirred at ambient temperature for 48 h. Then water amount was removed with a rotary evaporator for at least 8 h at 352 K. The unreacted amino acids were eliminated via precipitation in absolute ethanol. The synthesis AAPILs evaporated to remove ethanol undergo a vacuum for 5 h at 338 K. The water quantity of the AAPILs was determined about 0.01 in mass fractions using a Karl–Fischer titrator. ^{1}H NMR spectra of AAPILs are represented in the supplementary information (Figs. S3–S9).

Characterization of aminate anion AAPILs

To characterize the AAPILs after CO_2 absorption was used a spectrometer of FT-IR (Bruker, Tensor 27). Densities of the AAPILs were measured using the flotation method at 298.15 K in mixtures of chloroform and acetone. The mixture of the solution was adjusted so that the AAPIL remained suspended throughout. The density of the solutions was determined with a density analyzer (DSA5000, Anton Paar).

Gas absorption apparatus

QCM sensor was applied for gas absorption measurement. The cell of solubility entails an 8 MHz AT-cut quartz crystal utilized in the electrical oscillator circuit. Absorption apparatus

performance has been mentioned in the prior papers by authors in details [22–26]. The quantity of absorbed CO_2, $n_{CO_2}/n_{monomer}$ ($mol_{CO_2} \cdot mol^{-1}_{monomer}$) was computed as follows:

$$\frac{n_{CO_2}}{n_{monomer}} = \frac{\Delta F_S}{\Delta F_C} \times \frac{M_{monomer}}{M_{CO_2}} \quad (1)$$

where ΔF_C frequencies difference between the coated and the uncoated crystal. ΔF_S is the frequencies difference between the PILs covered crystal under vacuum and the PILs covered crystal after CO_2 adsorption.

Thermodynamic model

The data of absorption isotherm were fitted by the "deactivated model'' offered by Goodrich et al. [27] to describe the physical and chemical absorption of CO_2 in AAPILs. This model, the CO_2 amount absorbed in the AAPIL considers as the sum of two contribution (physical and chemical absorption) and assumes that only 1:1 reaction happens and less than 100% of the ionic liquids are allowed to react with CO_2. The mechanism of CO_2 physically and chemically absorption expressed as follows:

$$CO_{2(g)} \leftrightarrow CO_{2(l)} \quad (2)$$

$$\mathrm{AAIL}_{(l)} + CO_{2(l)} \xleftrightarrow{K_x} CO_2 - \mathrm{AAIL}_{(l)} \quad (3)$$

Henry's law is related to CO_2 physically absorption as follows:

$$p_{CO_2} = Hx_{CO_{2(l)}} \quad (4)$$

where $x_{CO_{2(l)}}$ is the physically absorption value, p_{CO_2} is the partial pressure of CO_2 in bar, H is the CO_2 Henry's law constant in the AAPILs in bar. The adsorbed CO_2 undergoes a reaction after physically absorption and the value of chemically absorbed CO_2 in the AAPILs is shown using the reaction equilibrium constant (K_x):

$$K_x = \frac{x_{CO_2-monomer_{(l)}}}{x_{monomer_{(l)}} x_{CO_{2(l)}}} \quad (5)$$

The total mole of the AAPIL monomers is the sum of the moles of the AAPIL monomer, $CO_2 - monomer$ complex and the deactivated the AAPIL monomers. The mole of the deactivated AAPIL monomer indicates the mole of the AAPIL monomers that does not react with CO_2.

$$n^0_{\text{monomer}} = n_{\text{monomer}} + n_{CO_2-monomer} + n_{deactivated-\text{monomer}} \quad (6)$$

The total mole of CO_2 in the AAPILs is the total absorbed CO_2 both physically and the chemically reacted as AAPIL–CO_2 complex,

$$n_{CO_2} = n_{CO_{2(l)}} + n_{CO_2-monomer_{(l)}} \quad (7)$$

The total mole of CO_2 in the AAPIL calculated from solving Eqs. (4), (5) and (6) as follows:

$$\frac{n_{CO_2}}{n^0_{\text{monomer}}} = \frac{p_{CO_2}}{H - p_{CO_2}} + \frac{K_x p_{CO_2}}{H + K_x p_{CO_2}}\left(1 - \frac{n_{deactivated-\text{monomer}}}{n^0_{monomer}}\right) \quad (8)$$

This model assumes that not all of the AAPIL monomers are available for reacting with the CO_2 molecule and $C = 1 - \frac{n_{deactivated-\text{monomer}}}{n^0_{monomer}}$ is considered as an experimental constant.

Result and Discussion

Physical Characterization of AAPILs

AAPILs' physical characterization is indicated in Table 2. Table 2 indicates the densities of AAPILs at temperature 298.15 K. The data imply that the structures of aminate-anion influence the densities of the PILs notably. It has been observed that the densities incremented as [Hist] > [Pro] > [Lys] > [Gly] > [Ala] > [Arg] > [Val]. Lengthen the alkyl side chains of [AA] increments the free volume of the PILs thereby decrementing their density. Moreover, the AAPILs with

aromatic rings [His] and [Pro] have a relatively high density compared to the other anions. The present AAPILs reveal a similar trend in densities as reported for AAILs having the same $[AA]^-$ anions with different cations [28–30].

Characterization of aminate P[VBIm][AA]s after CO_2 absorption

Obtained FT–IR spectra of the AAPILs: P[VBIm][Gly], P[VBIm][Ala], P[VBIm][Val], P[VBIm][Pro], P[VBIm][His], P[VBIm][Arg], and P[VBIm][Lys] after and before CO_2 absorption are illustrated in Fig. 1. The reaction between CO_2 and aminate anion of monomer produced carbamate. The characteristic FT-IR peaks related to C=O of the COO^- anion, which generally overlaps with –NH from the amino acids, were observed at 1550-1580 cm^{-1} with high intensity. Broad signals at 2825–3562 $cm^{-1}cm^{-1}$ related to –NH in secondary amides that resulted from CO_2 reacting with NH_2 and the peak of the C-N stretch was indicated at 1480 cm^{-1}. The peak with strong intensity at 1640-1650 cm^{-1} corresponding to the carbamate species. The reaction between CO_2 and NH_2 was confirmed in AAPILs. These functional groups confirmed the physical and chemical absorption in AAPILs.

Effect of pressure on CO_2 absorption

In this study, we investigated the absorption of CO_2 in the AAPILs with different aminates glycinate $[Gly]^-$, alaninate $[Ala]^-$, valinate $[Val]^-$, prolinate $[Pro]^-$, hisdinate $[His]^-$, lysinate $[Lys]^-$, and arginate $[Arg]^-$ at temperatures range of 288.15–308.15 K and pressures up to 5 bar. The absorption data of CO_2 in the AAPILs are reported in Table 3. To survey the effect of temperature and pressure, CO_2 absorption isotherms of the AAPILs with different aminates at different temperatures and pressures are displayed in Fig. 2. Fig. 2 indicates the dependence of absorption on pressure and temperature. CO_2 absorption in the AAPILs was incremented with increment in pressure and decrement in temperature. CO_2 absorption isotherms of the AAPILs

have a non-linear tendency and the CO_2 absorption rises a lot in the low-pressures while it enhancements nearly linearly in the higher pressures which represents more sensitivity of absorption to pressure in the low-pressure range. At low pressure, an increase of CO_2 absorption is related to the chemical absorption process, and the more increment at higher pressure corresponding to physical adsorption [31]. This behavior indicates that the CO_2 absorption in AAPILs at high pressure combines the chemical absorption and physical adsorption characteristic [32]. Brennecke et al. [33] reported the isotherms are subdivided into two distinct sections: a sharp increment at low pressures due to chemical absorption and a marginal increment in absorption capacity at higher pressures which is ordinary for physical absorption. Nonetheless, it was shown that the most of the capture was due to chemical absorption which results are in good agreement with our results reported. Also, a similar results are published for amino acid-based ILs, Raja Shahrom et al [34] reported that at low pressure, a high capture of CO_2 is owing to the chemical absorption process and the more increment at higher pressure is owing to physical adsorption. This behavior indicates that the CO_2 capture by AAPILs at high pressure merges the characteristics of physical adsorption as well as chemical absorption.

Effect of anion on CO_2 absorption

To survey the effect of anion, a comparison of CO_2 absorption in P[VBIm][Gly], P[VBIm][Ala], P[VBIm][Val], P[VBIm][Pro], P[VBIm][His], P[VBIm][Lys], and P[VBIm][Arg] is represented in Fig. 3. Fig. 3 demonstrates that CO_2 absorption rate of [Arg] with 1.05 mol/mol is higher, followed by [Lys], [Hist] have less CO_2 capacity with 0.95 mol/mol and 0.79 mol/mol, respectively. The [Arg] anion contains four amine groups; therefore, a higher chance for CO_2 is available to react with four accessible amine sites. [Lys] has the CO_2 absorption capacity lower than [Arg] and this behavior may be attributed to two primary amine groups in [Lys]. [His]

contains a pentagonal ring with one secondary and one primary amine groups; due to steric hindrance and low efficacies of secondary amine group [His] allocates third place after [Arg] and [Lys] (Fig. 3). [Pro], [Gly], [Ala], and [Val] have a lone one amine group and have a CO_2 capacity with 0.63, 0.60, 0.53, and 0.50 mol/mol respectively. The amine group number and alkyl chain length of cation are two main factors that effect on the process of CO_2 absorption. The results indicate that the effect of the amine group's number is more important than the alkyl chain length in the CO_2 absorption process. The remainder of the AAPILs ([Gly], [Ala], [Val]) have one primary amine group and a nonpolar aliphatic side chain. All these AAPILs display less or more similar capacities of CO_2 absorption as illustrated in Fig. 3. The obtained results are similar to available reports in the literature for monomeric (AAILs) and polymeric (AAPILs). Raja Shahrom et al [34] were investigated CO_2 absorption in forms of AAILs and AAPILs for eight anions [Gly], [Ala], [Ser], [Tau], [Arg], [Lys], [Hist], and [Pro] with ammonium based, [VBTMA], cation. They indicate that [VBTMA][Arg] gave the highest capacity of CO_2 absorption with 0.83 mol/mol and [VBTMA][Ala] has the least capacity of CO_2 absorption with 0.29 mol/mol. Also, they reveal P[VBTMA][Arg] and P[VBTMA][Lys] have higher CO_2 absorption with 1.14 mol/mol and 1.13 mol/mol respectively, P[VBTMA][Ala] has lowest absorption with 0.56 mol/mol. Sistla et al. [12] have been investigated various AAILs and observed that CO_2 absorption capacities were as order: [bmim][Arg] (0.62 mol CO_2/mol IL)> [bmim][Lys] (0.48 mol CO_2/mol IL) > [bmim][His] (0.45 mol CO_2/mol IL) > [bmim][Pro] (0.32 mol CO_2/mol IL). Santiago et al. [35] have been reported that [bmim][Met] and [bmim][Gly] present similar and the highest CO_2 sorption capacity (0.035 g CO_2/g IL), while [bmim][Pro] shows lower one (0.020 g CO_2/g IL). Also, the values of H and K_x increase in the order of [Arg] > [Lys] > [His] > [Gly] > [Ala] > [Val] > [Pro]. In Eq. (8) the primary term and second term

indicate physical absorption and chemical absorption, respectively. The high quantities of the chemical reaction constant (K_x) reveals that chemical absorption has seven contribution in the CO_2 absorption process while the higher values of Henry constant (H) reveals that physical absorption has low contribution in the CO_2 absorption process in AAPILs. Therefore, the high values of K_x represent a strong driving force in the formation complex of the AAPILs with CO_2.

Parameters of thermodynamic model

To achieve a deep understanding of the CO_2 absorption phenomenon in AAPILs, it is necessary to assess the contributions of chemical and physical individually. For this purpose, the experimental adsorption data were fitted by Eq. (8) by the non-linear regression and the thermodynamic parameters were calculated. The calculated experimental absorption data represent that the CO_2 absorption in the AAPILs is well correlated by Eq. (8) and CO_2 is absorbed both physically and chemically. In the CO_2 absorption process, the values of Henry's law constant (H) and the reaction equilibrium constants (K_x) are related to the CO_2 absorption capacity. The physical absorption is related to Henry's law constant (H), and the reaction equilibrium constant (K_x) is related to the chemical absorption. So, these parameters obtained by fitting the experimental absorption data and then evaluate the absorbent for the CO_2 absorption process. The fitted parameters Henry's constant (H), the reaction equilibrium constant (K_x), experiment constant (C), the correlation coefficient (R^2), and absolute average relative deviation ($AARD$) are summarized in Table 4. The results manifest that the correlation coefficients R^2 higher than 0.999 which implies to the applicably of the suggested model. According to Table 4, H values increment by incrementing temperature, while K_x values decremented at all the AAPILs. Also, the values of H and K_x increase in the order of [Arg] > [Lys] > [His] > [Pro] > [Gly] > [Val] > [Ala]. In Eq. (8) the primary term and second term indicate physical absorption

and chemical absorption, respectively. The high values of Henry constant (H) is related to the low physical control and the low values of the chemical reaction constant (K_x) is attributed to the chemical contribution.

Enthalpy of dissolution and reaction

The effect of temperature on CO_2 absorption is attributed to the molar enthalpy of absorption: [36–38]:

$$\Delta \mathrm{H}_{eq} = -R\left(\frac{\partial \ln K_X}{\partial(1/T)}\right) \tag{9}$$

$$\Delta \mathrm{H}_{sol} = R\left(\frac{\partial \ln H}{\partial(1/T)}\right) \tag{10}$$

The investigation demonstrates that increase of the temperature decrements the value of dissolved CO_2 which indicating the physical absorption of gas in the mixture and corresponding to the physical contribution (H values). Moreover, an rising temperature reduces CO_2 chemical absorption, i.e. K_x reduces at high temperatures which this behavior is in well agreement with usual exothermic reactions expressed in CO_2 absorption in ILs [39,40]. The values of enthalpy were assessed from plots of H_{CO2} and K_x against T, and the obtained data are reported in Table 5. The negative quantities of chemical reaction enthalpy (ΔH_{eq}) and physical dissolution enthalpy (ΔH_{sol}) expose that the CO_2 absorption process in the AAPILs is exothermic.

Regeneration efficiency of the AAPILs

Regeneration is one of the important factors to assess absorption efficiency. To evaluate the capacity of reuse, three cycles of CO_2 absorption/desorption trial of P[VBIm][Arg] investigated and plotted in Fig. 4. Fig. 4 demonstrates that the yield of the P[VBIm][Arg] is approximately constant after three consecutive recycles. For the regeneration experiment, CO_2 absorption is tested at 1 bar and 293.15 K, and desorption under vacuum at a temperature of 293.15 K and 90

min to omit CO_2. The absorption/desorption amount represents that CO_2 was perfectly omitted in 90 min and the absorption amount is stable in three cycles. The reduction in CO_2 absorption capacity of the regenerated P[VBIm][Arg] was apperceived to be about 1% in the three cycles of regeneration in comparison to the fresh sample. This behavior indicates that the P[VBIm][Arg] is regenerable and stable under practicable situations of regeneration. The CO_2 absorption quantities of P[VBIm][Arg] are obtained 0.587, 0.585, 0.585, 0.583, 0.599 and 0.599 in six sequential cycles of absorption/desorption and the regeneration yield P[VBIm][Arg] are 97.58%, respectively after three consecutive cycle absorption/desorption.

Conclusions

CO_2 absorption in the AAPILs has been evaluated in the temperature range 288.15–308.15 K and pressures up to 5 bar by QCM. The reaction equilibrium thermodynamic model has been utilized to assess chemical and physical absorption of CO_2 in the AAPILs. The outcomes reveal that the CO_2 absorption in the AAPILs at low pressures is generally attributed to chemical absorption. Various aminates with primary and secondary amines were considered to study the effect of the amino acid anion nature on CO_2 absorption capacity. Among of AAPILs investigated, P[VBIm][Arg] has the highest CO_2 absorption capacity and P[VBIm][Val] has the lowest CO_2 absorption capacity. This phenomenon reveals that the AAPILs with several amine sites represent higher CO_2 absorption capacity than the AAPILs with one primary amine group. The FT–IR spectroscopy of the CO_2 absorbed AAPILs indicates the formation of carbamate species. Also, the physical dissolution enthalpy and the chemical reaction show that the CO_2 absorption process in the AAPILs is exothermic.

Statements and Declaration

The authors declare that they have no known competing financial and non financial interest so personal relationships that could have appeared to influence the work reported in this paper.

References

1. Firaha DS, Kirchner B (2016) Tuning the carbon dioxide absorption in amino acid ionic liquids, ChemSusChem. 9:1–10.

2. Lei Z, Dai C, Chen B(2014) Gas solubility in ionic liquids, Chem. Rev. 114: 1289–1326.

3. Pan M, Wang C (2015) Recent advances in CO_2 capture by functionalized ionic liquids, advances in CO_2 capture, sequestration, and conversion, American Chemical Society, Washington, DC, 1194: 341–369.

4. Matter JM, Stute M, Snaebjornsdottir SO, Oelkers EH, Gislason SR, Aradottir ES, Sigfusson B, Gunnarsson I, Sigurdardottir H, Gunnlaugsson E, Axelsson G, Alfredsson HA, Wolff-Boenisch D, Mesfin K, Taya DFDlR, Hall J, Dideriksen K, Broecker WS (2016) Rapid carbon mineralization for permanent disposal of anthropogenic carbon dioxide emissions,Science 352: 1312–1314.

5. Rochelle GT (2009) Amine scrubbing for CO_2 capture, Science 325 : 1652–1654.

6. Cui GK, Wang JJ, Zhang SJ (2016) Active chemisorption sites in functionalized ionic liquids for carbon capture, Chem. Soc. Rev. 45 : 4307–4339.

7. Earle MJ, Esperanca J, Gilea MA, Lopes JNC, Rebelo LPN, Magee JW, Seddon KR, Widegren JA (2006) The distillation and volatility of ionic liquids, Nature, 439 : 831–834.

8. MacDowell N, Florin N, Buchard A, Hallett J, Galindo A, Jackson G, Adjiman CS, Williams CK, Shah N, Fennell P (2010) An overview of CO_2 capture technologies, Energy Environ. Sci. 3:1645–1669.

9. Bara JE, Camper DE, Gin DL, Noble RD (2010) Room-temperature ionic liquids and composite materials: platform technologies for CO_2 capture, Acc. Chem. Res. 43: 152–159.

10. Vidal L, Riekkola ML, Cannals A (2012) Ionic liquid-modified materials for solid-phase extraction and separation : a review, Anal. Chim. Acta 715 : 19–41.

11. Bates ED,. Mayton RD, Ntai I, Davis JH (2002) CO_2 capture by a Task-Specific ionic liquid. J. Am. Chem. Soc., 124 : 926–927.

12. Sistla YS, Khanna A (2014) CO_2 absorption studies in amine functionalized ionic liquids, J. Ind. Eng. Chem. 20 : 2497–2509.

13. Saravanamurugan Sh., Kunov-Kruse AJFR, Riisager A (2014) Amine-Functionalized Amino acid-based ionic liquids as efficient and high-capacity absorbents for CO_2, ChemSusChem. 7 : 897-902.

14. Tang J, Sun W, Tang H, Radosz M, Shen Y (2005) Enhanced CO_2 Absorption of Poly(ionic liquid)s, Macromolecules, 38 : 2037-2039.

15. Tang J, Tang H, Sun W, Radosz M, Shen Y(2005) Low-pressure CO_2 sorption in ammonium-based poly(ionic liquid)s, Polymer, 46 : 12460-12467.

16. Raja Shahrom M Sh, Wilfred C D, Ziyada Taha A Kh (2016) CO_2 capture by task specific ionic liquids (TSILs) and polymerized ionic liquids (PILs and AAPILs), J. Mol. Liq. 219 : 306–312

17. Yu CH (2012) A Review of CO_2 Capture by Absorption and Adsorption, Aerosol and Air Quality Research.

18. Privalova EI, Karjalainen E, Nurmi M, Maki-Arvela P, Eranen K, Tenhu H, Murzin D Yu, Mikkola JP (2013) Imidazolium-based poly(ionic liquid)s as new alternatives for CO_2 capture, ChemSusChem. 6 : 1500-1509.

19. Amajjahe S, Ritter H (2008) Anion Complexation of Vinylimidazolium Salts and Its Influence on Polymerization, Macromolecules, 41: 716 –718.

20. Muldoon MJ, Gordon CM (2004) Synthesis of gel-type polymer beads from ionic liquid monomers, J. Polym. Sci. Part A: Polym. Chem. 42 : 3865– 3869.

21. Mori H,. Yahagi M, Endo T (2009) RAFT Polymerization of N-vinylimidazolium salts and synthesis of thermoresponsive ionic liquid block copolymers, Macromolecules 42 : 8082–8092.

22. Noorani N, Mehrdad A (2021) Experimental and theoretical study of CO_2 sorption in biocompatible and biodegradable cholinium-based ionic liquids,) Sep. Purif. Technol. 254 : 117609.

23. Noorani N, Mehrdad A (2020) CO_2 solubility in some amino acid-based ionic liquids: Measurement,correlation and DFT studies, Fluid Phase Equilibria 517 :112591.

24. Mehrdad A, Noorani N (2019) Study of CO_2 adsorption onto poly(1–vinylimidazole) using quartz crystal microbalance and density functional theory methods. J. Mol. Liq. 291: 111288.

25. Noorani N, Mehrdad A (2019) Adsorption, permeation, and DFT studies of PVC/PVIm blends for separation of CO_2/CH_4, J. Mol. Liq. 292 : 111410.

26. Noorani N, Mehrdad A (2020) Modification of PVC with 1-Vinylimidazole for CO_2/CH_4 Separation: Sorption, Permeation and DFT Studies, Phys. Chem. Res. 8 : 689–703.

27. Moya C, Alonso-Morales N, Riva J, Morales-Collazo O, Brennecke JF, Palomar J, (2018) Encapsulation of ionic liquids with an aprotic heterocyclic anion (AHAIL) for CO_2 capture: preserving the favorable thermodynamics and enhancing the kinetics of absorption, J. Phys. Chem. B 122 : 2616–2626.

28. Sudha Sistla Y, Khanna A (2015) CO_2 Absorption Studies in Amino Acid-Anion Based Ionic Liquids.Chem.Eng.J. 273 : 268-276.

29. Muhammad N, Man Z B, Azmi Bustam M, Abdul Mutalib M I, Wilfred CD, Rafiq S (2011) Synthesis and Thermophysical Properties of Low Viscosity Amino Acid-Based Ionic Liquids. J. Chem. Eng. Data 56 : 3157–3162.

30. Zhang Y, Zhang S, Lu X, Zhou Q, Fan W, Zhang XP (2009) Dual Amino-Functionalised Phosphonium Ionic Liquids for CO2 Capture. Chem. Eur. J. 15 : 3003 – 3011.

31. Goodrich B F, Fuente JCd, Gurkan BE, Zadigian DJ, Price EA, Huang Y, Brennecke J F (2011) Experimental measurements of amine-functionalized anion-tethered ionic liquids with carbon dioxide, Ind. Eng. Chem. Res. 50 : 111–118.

32. Torralba-Calleja E, Skinner J, Gutierrez-Tauste D(2013) CO_2 capture in ionic liquids: a review of solubilities and experimental methods, J. Chem. 2013 : 1–16.

33. Gurkan BE, de la Fuente JC, Mindrup EM, Ficke LE, Goodrich BF, Price EA, Schneider, J.F. Brennecke WF(2010) Equimolar CO_2 absorption by anion-functionalized ionic liquids, J. Am. Chem. Soc. 132 : 2116–2117.

34. Raja Shahrom M Sh, Wilfred CD, MacFarlane DR,. Vijayraghavan R, Kait Ch F (2019) Amino acid based poly(ionic liquid) materials for CO_2 capture: Effect of anion, J. Mol. Liq. 25 : 644-652.

35. Santiago R, Lemus J, Moya Ch, Moreno D, Alonso-Morales N, Palomar J (2018) Encapsulated Ionic Liquids to enable the practical application of amino acid-based Ionic Liquids in CO_2 capture, ACS Sustainable Chem. Eng. 6 : 14178–14187.

36. Chen YF, Zhang YY, Yuan SJ, Ji XY, Liu C, Yang ZH, Lu XH (2016) Thermodynamic study for gas absorption in choline-2-pyrrolidine-carboxylic acid+ polyethylene glycol, J. Chem. Eng. Data 61: 3428–3437.

37. Huang K, Zhang XM, Hu XB, Wu YT (2016) Hydrophobic protic ionic liquids tethered with tertiary amine group for highly efficient and selective absorption of H_2S from CO_2, AlChE J. 62: 4480–4490.

38. Zhou ZM, Jing GH, Zhou LJ(2012) Characterization and absorption of carbon dioxide into aqueous solution of amino acid ionic liquid [N_{1111}][Gly] and 2-amino-2-methyl-1-propanol, Chem. Eng. J. 204 : 235–243.

39. Zoubeik M, Henni A (2014) Experimental and thermodynamic study of CO_2 solubility in promising [TF2N and DCN] ionic liquids, Fluid Phase Equilib. 376 : 22–30.

40. Kurnia KA, Harris F, Wilfred CD, Mutalib MIA, Murugesan T (2009) Thermodynamic properties of CO_2 absorption in hydroxyl ammonium ionic liquids at pressures of (100–1600) kPa, J. Chem. Thermodyn. 41: 1069–1073.

41. McMurry J (2011) Fundamentals of Organic Chemistry, seventh ed., Cengage Learning, USA, pp. 506–507.

Table 1. Properties and molecular structures of amino acids [38].

Amino acid	Abbreviation	Molecule weight	pK_a (α-NH_3^+)	Molecular structure
Glycine	Gly	75.07	9.60	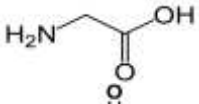
L–Alanine	Ala	89.09	9.87	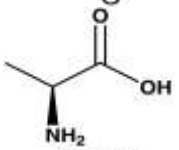
L–Valine	Val	117.15	9.62	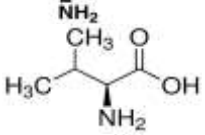
L–Proline	Pro	115.13	10.60	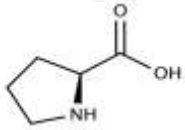
L–Histidine	His	155.15	9.17	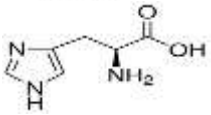
L–Lysine	Lys	146.19	8.95	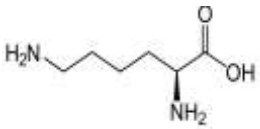
L–Arginine	Arg	174.20	9.04	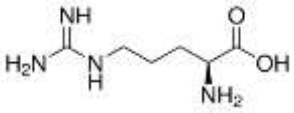

Table 2. Physical properties of AAPILs synthesized.

AAPILs	Density	Color	Form
P[VBIm][Gly]	1.09962	Yellowish	Solid
P[VBIm][Ala]	1.02639	Yellowish	Solid
P[VBIm][Val]	0.99676	Whitish	Solid
P[VBIm][Pro]	1.12680	Brownish	Solid
P[VBIm][His]	1.15386	Brownish	Solid
P[VBIm][Lys]	1.10997	Yellowish	Solid
P[VBIm][Arg]	0.99946	Yellowish	Solid

Table 3. CO_2 absorption capacity $n_{CO2}/n_{monomer}$ of AAPILs in the temperature range 288.15–308.15 K and pressure up to 5 bar.

T = 288.15K		T = 298.15K		T = 308.15K	
P /bar	$mol_{CO_2}/mol_{monomer}$	P /bar	$mol_{CO_2}/mol_{monomer}$	P /bar	$mol_{CO_2}/mol_{monomer}$
			P[VBIm][Arg]		
0.2098	0.1663	0.2069	0.1515	0.2151	0.1056
0.3787	0.2758	0.4661	0.2826	0.4251	0.1919
0.5768	0.3678	0.6571	0.3547	0.7929	0.332
0.8336	0.4675	0.9208	0.4304	1.0836	0.3953
0.9488	0.4949	1.5000	0.5689	1.5000	0.5047
1.5000	0.6279	2.0000	0.6576	2.0000	0.593
2.0000	0.7062	2.5000	0.7297	2.5000	0.6621
2.5000	0.8001	3.0000	0.7943	3.0000	0.7389
3.0000	0.8470	3.5000	0.8460	3.5000	0.7964
3.5000	0.9116	4.0000	0.9051	4.0000	0.8598
4.0000	0.9683	4.5000	0.9550	4.5000	0.8982
4.5000	1.0094	5.0000	1.0067	5.0000	0.9365
5.0000	1.0583				
			P[VBIm][Lys]		
0.2449	0.2744	0.1825	0.1120	0.2069	0.1322
0.4903	0.4209	0.3130	0.1864	0.3593	0.1913
0.7070	0.4953	0.5350	0.2778	0.6014	0.2887
0.9561	0.5725	0.8099	0.3797	1.0438	0.4278
1.5000	0.6744	0.9966	0.4255	1.5000	0.5043
2.0000	0.7411	1.5000	0.5345	2.0000	0.5669
2.5000	0.7903	2.0000	0.6224	2.5000	0.6087
3.0000	0.836	2.5000	0.6716	3.0000	0.6435
3.5000	0.8781	3.0000	0.7278	3.5000	0.6956
4.0000	0.9168	3.5000	0.7735	4.0000	0.7548
4.5000	0.9378	4.0000	0.8157	4.5000	0.7791
5.0000	0.9554	4.5000	0.8579	5.0000	0.8174
		5.0000	0.9107		
			P[VBIm][His]		
0.1337	0.1251	0.1120	0.0796	0.2069	0.1039
0.2613	0.2057	0.3173	0.1867	0.3730	0.145
0.5213	0.3113	0.6411	0.2937	0.6543	0.2106
1.0032	0.4335	0.9794	0.3651	1.0247	0.2872
1.5000	0.5114	1.5000	0.4365	1.5000	0.3392
2.0000	0.5614	2.0000	0.4969	2.0000	0.3912
2.5000	0.6058	2.5000	0.5353	2.5000	0.4377
3.0000	0.6475	3.0000	0.571	3.0000	0.4732
3.5000	0.6892	3.5000	0.6094	3.5000	0.5088
4.0000	0.7253	4.0000	0.6369	4.0000	0.5361
4.5000	0.7559	4.5000	0.6671	4.5000	0.5635
5.0000	0.792	5.0000	0.6918	5.0000	0.5963
			P[VBIm][Pro]		
0.1988	0.0870	0.2069	0.1072	0.1852	0.068
0.3785	0.1553	0.3784	0.1571	0.3867	0.1225
0.5876	0.2013	0.5874	0.1997	0.5738	0.1711
0.7843	0.2535	0.7925	0.2411	0.7615	0.208
0.9816	0.2833	0.9808	0.2655	0.9816	0.245
1.5000	0.3653	1.5000	0.3361	1.5000	0.3033
2.0000	0.4262	2.0000	0.3860	2.0000	0.348
2.5000	0.4796	2.5000	0.4287	2.5000	0.3947
3.0000	0.5243	3.0000	0.4615	3.0000	0.4316

3.5000	0.5529	3.5000	0.4993	3.5000	0.4569
4.0000	0.5840	4.0000	0.5249	4.0000	0.4958
4.5000	0.6138	4.5000	0.559	4.5000	0.5152
5.0000	0.6337	5.0000	0.5967	5.0000	0.5288
			P[VBIm][Gly]		
0.2204	0.0881	0.1364	0.0631	0.1201	0.0377
0.4578	0.1506	0.3791	0.1277	0.3866	0.1193
0.6514	0.197	0.5519	0.1719	0.6041	0.1664
1.2590	0.2979	0.9571	0.2523	1.0148	0.2371
1.5000	0.3332	1.5000	0.3201	1.5000	0.2920
2.0000	0.3893	2.0000	0.3706	2.0000	0.3376
2.5000	0.4245	2.5000	0.4179	2.5000	0.3831
3.0000	0.4677	3.0000	0.4494	3.0000	0.4114
3.5000	0.4966	3.5000	0.4872	3.5000	0.4506
4.0000	0.5382	4.0000	0.5172	4.0000	0.4836
4.5000	0.5655	4.5000	0.5487	4.5000	0.5040
5.0000	0.6023	5.0000	0.5708	5.0000	0.537
			P[VBIm][Ala]		
0.3075	0.1129	0.1662	0.0499	0.2204	0.0596
0.4909	0.1580	0.4248	0.1179	0.5597	0.1398
0.6935	0.2055	0.6011	0.161	0.7357	0.1696
0.9812	0.2574	0.9828	0.2222	0.9962	0.204
1.5000	0.3206	1.5000	0.2857	1.5000	0.2682
2.0000	0.3635	2.0000	0.3288	2.0000	0.3117
2.5000	0.3928	2.5000	0.3696	2.5000	0.353
3.0000	0.4380	3.0000	0.4036	3.0000	0.3805
3.5000	0.4673	3.5000	0.4331	3.5000	0.4057
4.0000	0.4944	4.0000	0.4648	4.0000	0.4355
4.5000	0.5283	4.5000	0.4875	4.5000	0.4653
5.0000	0.5441	5.0000	0.5192	5.0000	0.4813
			P[VBIm][Val]		
0.2014	0.0832	0.2123	0.0559	0.0474	0.0499
0.3921	0.1248	0.4057	0.1056	0.0804	0.0789
0.5819	0.1602	0.5957	0.1366	0.1113	0.1086
0.7839	0.2038	0.7811	0.1677	0.1319	0.1329
0.9777	0.2413	0.9900	0.1987	0.1546	0.1554
1.5000	0.2912	1.5000	0.2629	0.1958	0.2024
2.0000	0.3328	2.0000	0.3064	0.2349	0.2385
2.5000	0.3681	2.5000	0.3436	0.2659	0.2692
3.0000	0.3952	3.0000	0.3767	0.2988	0.2963
3.5000	0.4326	3.5000	0.4057	0.3215	0.321
4.0000	0.4451	4.0000	0.4368	0.3483	0.344
4.5000	0.4846	4.5000	0.4678	0.3668	0.3656
5.0000	0.5012	5.0000	0.4885	0.3854	0.3863

[a]Standard uncertainties are $u_r(n_{CO_2}/n_{AAIL}) = 0.001$, $u(T) = 0.05$ K, and $u(p) = 0.0010$ bar

Table 4. Henry's law constant (H), reaction equilibrium constant (K_x), experiment constant (C), the correlation coefficient (R^2) and absolute average relative deviation ($AARD$) for CO_2 absorption AAPILs at different temperatures (T).

AAPILs	T / K	H (bar)	K_x (bar^{-1})	C	R^2	[a]$AARD\%$
	288.15	12.67 ± 1.09	0.89± 0.72	0.97	0.9995	1.28
P[VBIm][Arg]	298.15	15.07± 1.02	0.81± 0.87	0.90	0.9997	0.99
	308.15	18.60 ± 1.88	0.77± 0.90	0.61	0.9992	1.46
	288.15	15.51 ± 0.78	0.71 ± 0.92	0.99	0.9996	1.29
P[VBIm][Lys]	298.15	17.12 ± 1.59	0.70 ± 0.77	0.97	0.9984	1.15
	308.15	21.23 ± 1.39	0.67± 1.05	0.91	0.9985	1.15
	288.15	18.04 ± 0.92	0.57 ± 1.25	0.94	0.9999	0.31
P[VBIm][His]	298.15	21.82 ± 1.26	0.52 ± 1.33	0.61	0.9998	1.16
	308.15	23.84 ± 1.75	0.45± 1.61	0.96	0.9990	1.23
	288.15	22.76 ± 2.03	0.51± 1.27	0.95	0.9989	1.49
P[VBIm][Pro]	298.15	24.27± 1.66	0.45± 1.71	0.99	0.9982	1.37
	308.15	25.33 ± 1.46	0.41± 1.53	0.99	0.9989	1.51
	288.15	22.87± 2.24	0.48 ± 1.14	0.75	0.9990	1.44
P[VBIm][Gly]	298.15	24.36 ± 0.93	0.44 ± 1.68	0.94	0.9996	1.42
	308.15	25.57 ± 1.03	0.40± 1.28	0.99	0.9989	1.06
	288.15	25.69 ± 1.29	0.43 ± 1.51	0.94	0.9996	1.31
P[VBIm][Ala]	298.15	26.22 ± 1.55	0.39 ± 1.31	0.93	0.9999	1.18
	308.15	28.06 ± 1.35	0.37± 1.44	0.91	0.9998	1.17
	288.15	26.26 ± 2.15	0.38 ± 1.80	0.98	0.9996	1.35
P[VBIm][Val]	298.15	27.27± 1.45	0.38± 1.45	0.79	0.9998	0.95
	308.15	32.44 ± 1.92	0.29± 1.86	0.75	0.9993	1.44

[a] $AARD\% = \frac{100}{n}\sum\left|\frac{x_{CO_2}^{cal} - x_{CO_2}^{\exp}}{x_{CO_2}^{\exp}}\right|$

Table 5. The enthalpy of physical absorption (ΔH_{sol}) and the enthalpy of chemical absorption (ΔH_{eq}) of CO_2 in AAPILs.

AAPILs	ΔH_{sol} /kJ·mol^{-1}	ΔH_{eq} /kJ·mol^{-1}
P[VBIm][Arg]	-14.12 ± 0.13	-5.36 ± 0.10
P[VBIm][Lys]	-11.53 ± 0.33	-2.13± 0.08
P[VBIm][His]	-9.45 ± 0.18	-8.69 ± 0.16
P[VBIm][Pro]	-3.95 ± 0.05	-8.06 ± 0.06
P[VBIm][Gly]	-4.12 ± 0.03	-6.70 ± 0.15
P[VBIm][Ala]	-3.24 ± 0.13	-5.56 ± 0.10
P[VBIm][Val]	-7.77 ± 0.27	-9.86 ± 0.72

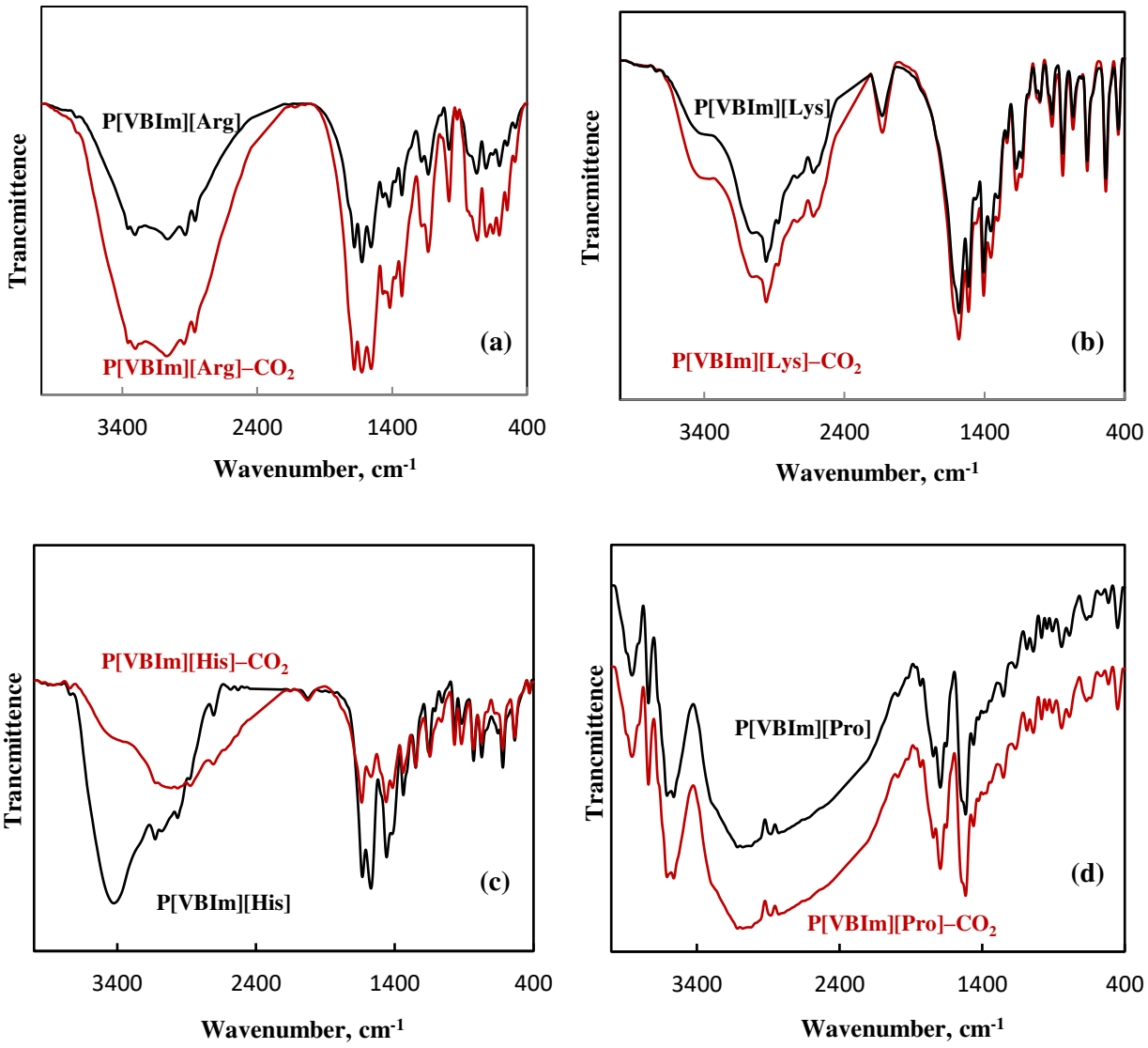
Trancmittence
P[VBIm][Arg]
P[VBIm][Arg]–CO2
(a)
3400
2400
1400
400
Wavenumber, cm-1
Trancmittence
P[VBIm][Lys]
P[VBIm][Lys]–CO2
(b)
3400
2400
1400
400
Wavenumber, cm-1
Trancmittence
P[VBIm][His]–CO2
P[VBIm][His]
(c)
3400
2400
1400
400
Wavenumber, cm-1
Trancmittence
P[VBIm][Pro]
P[VBIm][Pro]–CO2
(d)
3400
2400
1400
400
Wavenumber, cm-1

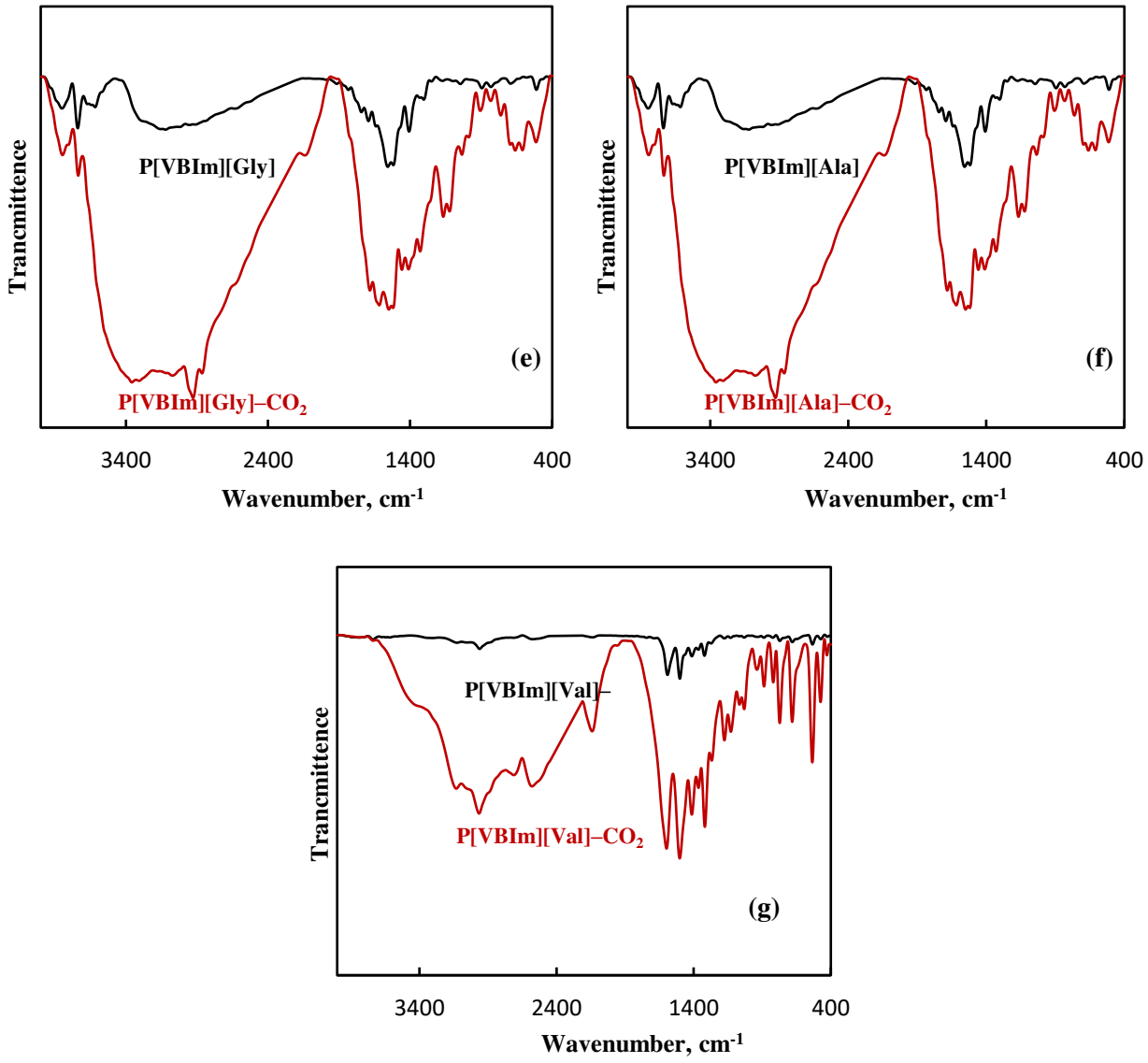

Fig. 1. FT–IR of AAPILs before and after CO_2 absorption.

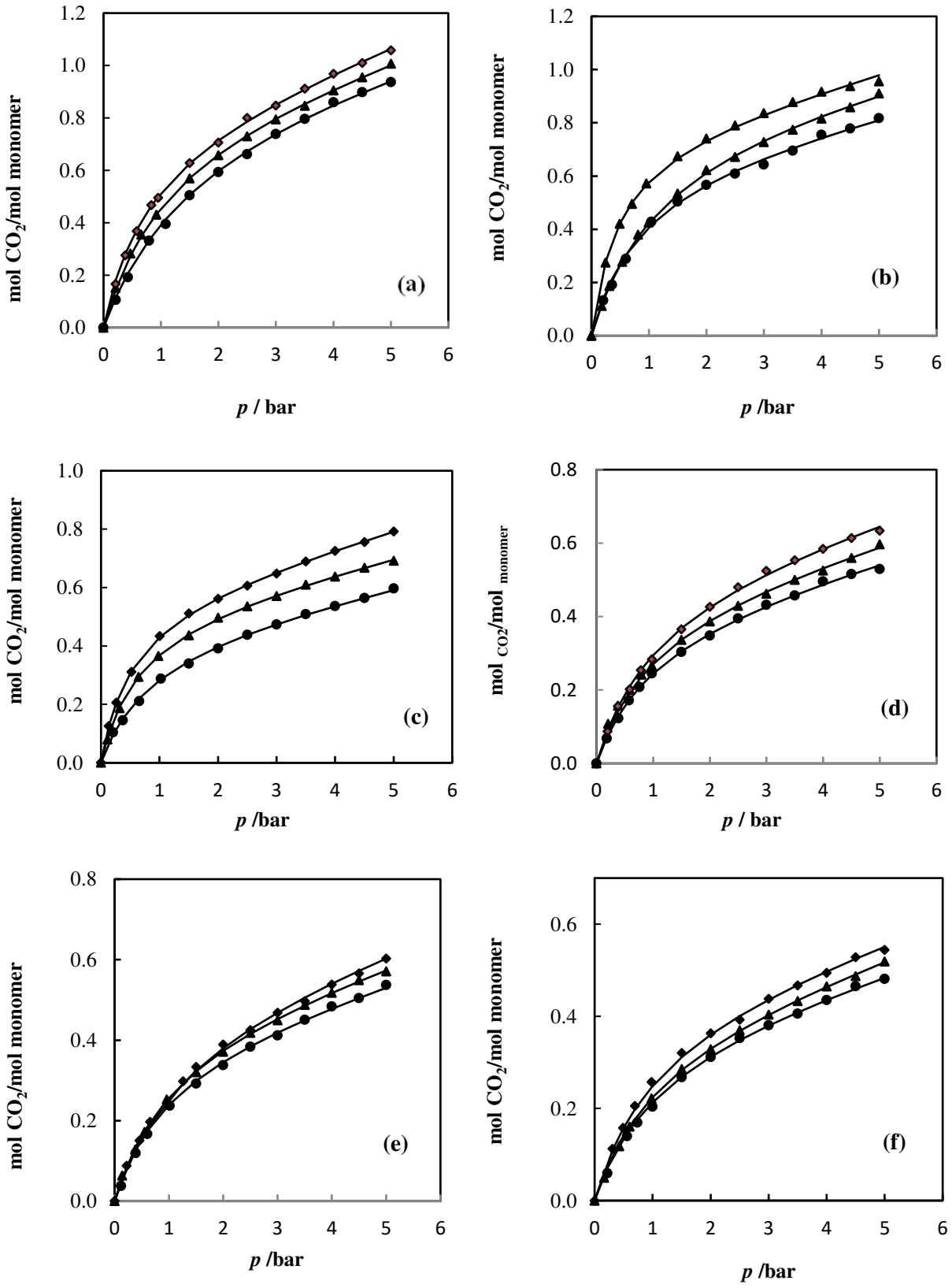
mol CO2/mol monomer
p / bar
(a)
(b)
(c)
(d)
(e)
(f)

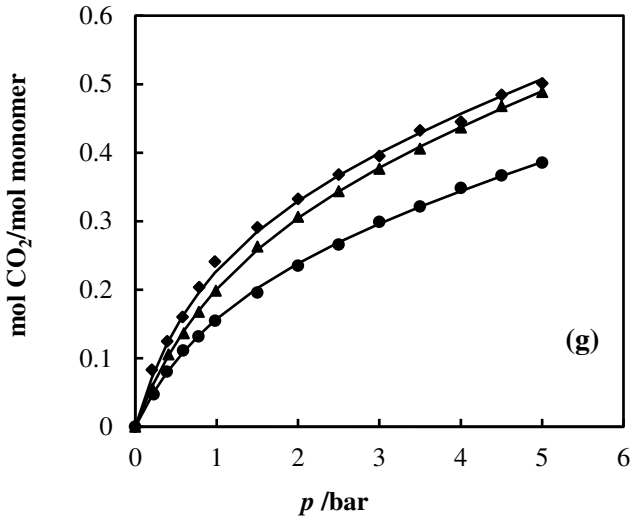

Fig. 2. The CO_2 absorption in (a) P[VBIm][Arg]; (b) P[VBIm][Lys]; (c) P[VBIm][His]; (d) P[VBIm][Pro]; (e) P[VBIm][Gly]; (f) P[VBIm][Ala]; (g) P[VBIm][Val] at different temperatures (♦) 288.15 K; (▲) 298.15 K; (●) 308.15 K; (–) Fitting results by Eq. (8).

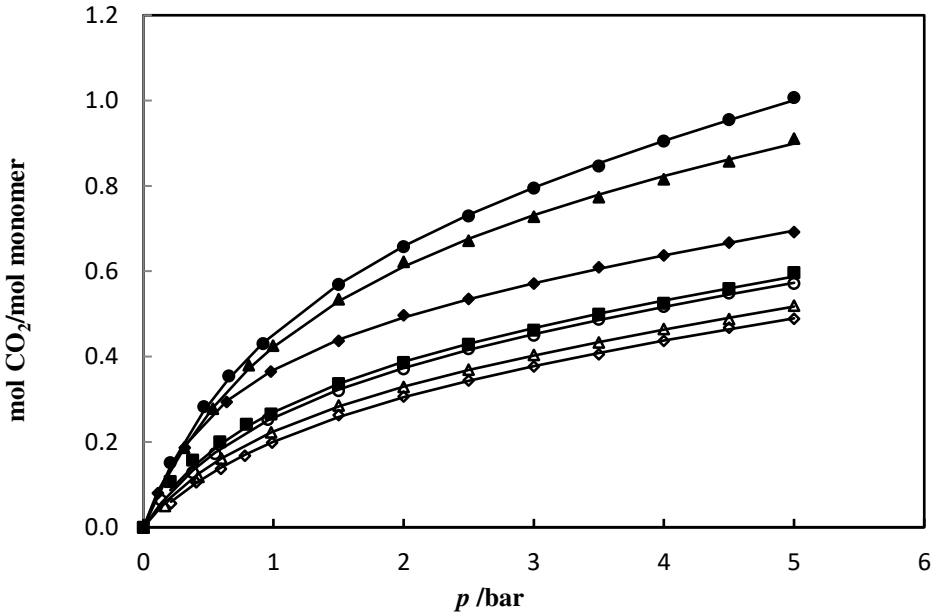

Fig. 3. . The CO_2 absorption in (●) P[VBIm][Arg]; (▲) P[VBIm][Lys]; (♦) P[VBIm][His]; (■) P[VBIm][Pro]; (○) P[VBIm][Gly]; (Δ) P[VBIm][Ala]; (◊) P[VBIm][Val] at temperatures 298.15 K; (–) Fitting results by Eq. (8).

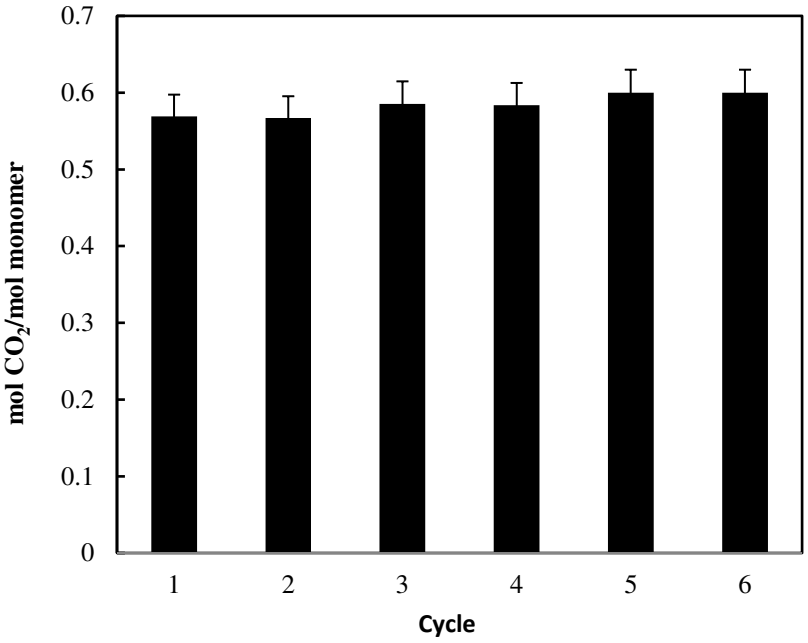

Fig. 4. The CO_2 absorption capacity of P[VBIm][Arg] at p = 1 bar and T = 298.15 K in six absorption/desorption cycles.